Earth and Planetary Science Letters 531 (2020) 115986

Contents lists available at ScienceDirect

Earth and Planetary Science Letters

www.elsevier.com/locate/epsl

Migration of shallow and deep slow earthquakes toward the locked segment of the Nankai megathrust

Naoki Uchida [a,*], Ryota Takagi [a], Youichi Asano [b], Kazushige Obara [c]

[a] *Graduate School of Science, Tohoku University, 6-6 Aramaki-aza-aoba, Aoba-ku, Sendai 980-8578, Japan*
[b] *National Research Institute for Earth Science and Disaster Resilience, 3-1 Tennodai, Tsukuba, Ibaraki 305-0006, Japan*
[c] *Earthquake Research Institute, University of Tokyo, Bunkyo, Tokyo 113-0032, Japan*

ARTICLE INFO

Article history:
Received 17 April 2019
Received in revised form 9 November 2019
Accepted 24 November 2019
Available online 6 December 2019
Editor: M. Ishii

Keywords:
slow earthquake
Nankai earthquake
slow slip
repeating earthquake
southwestern Japan subduction zone
preseismic slip

ABSTRACT

The Nankai megathrust is located offshore Shikoku and Kyushu, Japan and is characterized by various kinds of slow earthquakes whose relative motions across the plate boundary faults are slower than regular earthquakes. In the area, the interplate locking is stronger in the northern area (offshore Shikoku) than in the southern area (offshore Kyushu) and Mw ∼8 earthquakes (Nankai earthquakes) have occurred repeatedly in the northern area. In this paper, the spatio-temporal distributions of slow earthquakes (very low frequency earthquakes, tremors and slow-slip events) are examined based on the analyses of repeating earthquakes and slow earthquakes with special focus on the interaction between different activities. A comprehensive analysis of the seismic and geodetic data from 2003 to 2016 indicates complementary distribution of various types of slow earthquakes down to 35–50 km depth outside the Nankai main locking area. We also found interactions between different kinds of activities. The interactions between the repeating earthquakes and slow earthquakes suggest that the area of the repeating earthquakes activity can be divided into deeper (depth $\geq$ 20 km) and shallower (depth $<$ 20 km) areas. The analyses of deep repeating earthquakes and the inland Global Navigation Satellite System (GNSS) data suggests slow northward migrations of long-term slow slip events (SSEs) in 20–50 km (offshore Kyushu) and 20–35 km (under Shikoku) depths along the plate boundary. These migrations occurred during a period of 2–3 years that includes the 2003 and 2010 large slow-slip events in the Bungo channel located in between Kyushu and Shikoku. The analysis has also shown interaction between shallow repeating earthquakes and shallow very low frequency earthquakes which indicates faster northward migrations of short-term SSEs from the shallow plate boundary offshore Kyushu to the deeper area under Shikoku over the duration of a month during the 2010 long-term slow-slip episode. The deep slow migration and the shallow to deep fast migration of SSEs in a ∼300 km area towards and around the source area of the recurrent Nankai earthquake (Mw 8.0–8.6) indicates the occurrence of a widespread non-steady stress build-up process around the source area of the Nankai megathrust earthquake.

1. Introduction

The slow earthquakes such as the nonvolcanic tremors, the very low frequency earthquakes (VLFEs), and the short- and long-term slow-slip events (SSEs) are major non-steady processes that release the stress accumulated in the megathrust zone significantly slower than the regular earthquakes (e.g., Beroza and Ide, 2011; Bürgmann, 2018; Hirose and Obara, 2005; Obara and Kato, 2016). The slow and regular earthquakes with different time constants are sometimes located in the neighboring regions of a fault (e.g., Beroza and Ide, 2011; Obara and Kato, 2016). Such slow earthquakes are characterized by episodic stress release in the area adjacent to locked seismogenic areas and may temporarily increase stress and earthquake probabilities in the locked areas (Mazzotti and Adams, 2004; Uchida et al., 2016). The slow earthquakes also have the potential to become the nucleation phase of eventual megathrust earthquakes (Matsuzawa et al., 2010; Segall and Bradley, 2012). Previous studies have suggested that slow defor-

* Corresponding author at: Research Center for Prediction of Earthquakes and Volcanic Eruptions, Graduate School of Science, Tohoku University, 6-6 Aramaki-aza-aoba, Aoba-ku, Sendai 980-8578, Japan.
E-mail address: naoki.uchida.b6@tohoku.ac.jp (N. Uchida).

https://doi.org/10.1016/j.epsl.2019.115986

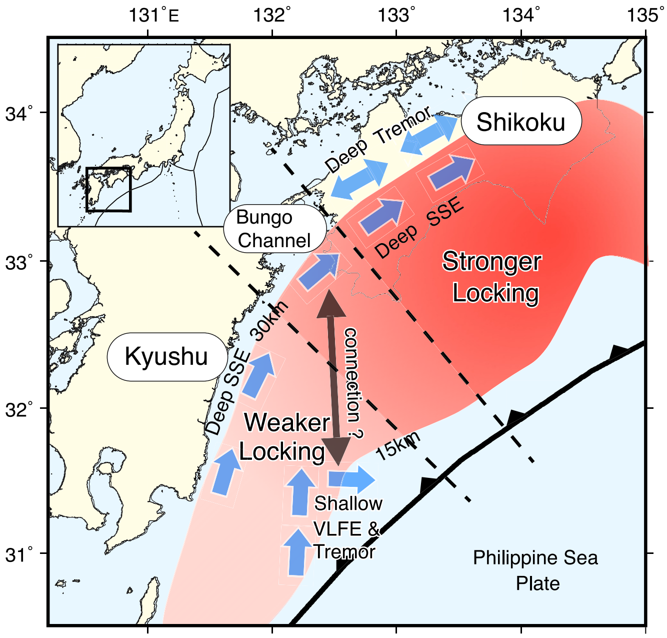

Fig. 1. Schematic showing interplate locking (red) and migration directions (arrows) of SSEs and slow earthquakes along the southern Nankai trough region as detected by previous studies (Asano et al., 2015; Obara, 2010; Takagi et al., 2016; Yamashita et al., 2015). The dashed line is the boundary of the region. The Bungo channel is located in the transitional area. (For interpretation of the colors in the figure(s), the reader is referred to the web version of this article.)

mation and its migration can occasionally precede major earthquakes (Graham et al., 2014; Kato et al., 2012; Mavrommatis et al., 2015; Meng et al., 2015; Radiguet et al., 2016; Roeloffs, 2006; Uchida et al., 2016; Voss et al., 2018). Therefore, the interaction and relationship between slow and megathrust earthquakes is one of important global problems even though many slow earthquakes have been ubiquitously detected in many places around the world.

A large interplate slip deficit along the offshore Shikoku segment of Nankai trough, southwest Japan (Figs. 1 and 2d) (e.g., Nishimura et al., 2018; Yokota et al., 2016) has become a seismic source area of the recurrent M8.0–8.6 interplate earthquakes, including the 1946 Nankai earthquake (Mw ∼8.1, Fig. 2c) (Ando, 1975; Sagiya and Thatcher, 1999). Conversely, no Mw ∼8 earthquakes have been detected in the area offshore Kyushu which is characterized by moderate to small interplate earthquakes as well as active small repeating earthquakes (Yamashita et al., 2012). These results suggest relatively strong and weak interplate locking in the northern (Shikoku) and southern (Kyushu) areas, respectively (Fig. 1). The repeating earthquakes and other slow earthquakes in the relatively weak locking area also provide information on temporal change of slow slip. However, the temporal change of repeating earthquake activity, which is an indicator of slow slip in the seismogenic depth of the plate boundary, has not been investigated before in this area.

In this study, we identify small repeating earthquakes (hereafter repeaters) that are located in the depth range between the deep nonvolcanic tremors and shallow VLFEs. Then the activities of repeaters, catalogs of deep nonvolcanic tremors, shallow VLFEs, and long-term SSEs based on the time series of Global Navigation Satellite System (GNSS) data are all used to understand the interaction of slow earthquakes. They have also been employed to characterize slow and fast migration of interplate creep along deeper and shallower plate boundary of the Nankai trough subduction zone that probably show that large plate-boundary area is behaving as a single system.

2. Data and method

2.1. Repeaters

The repeaters have nearly identical waveforms and are characterized by the repeated rupture of a small seismic patch surrounded by the creeping area (Nadeau and Johnson, 1998; Uchida and Bürgmann, 2019; Uchida and Matsuzawa, 2013) (Fig. 3). Several studies have postulated that the seismic slip of repeaters are indicative of fault creep in the surrounding area of the repeaters, thereby making suitable for the estimation of the interplate creep rate, especially in the offshore areas (Igarashi et al., 2003; Mavrommatis et al., 2015; Uchida et al., 2016) (Fig. 3). In this study, repeaters were identified for the period from April 2002 to July 2015 in the Nankai megathrust zone by using the method reported by Uchida and Matsuzawa (2013) who utilized waveform similarity of repeaters. Here, waveforms data obtained from the High-Sensitivity Seismograph Network (Hi-net) (National Research Institute for Earth Science and Disaster Resilience, 2019a) are used to calculate coherence for earthquakes with M $\geq$ 2.0 detected by the Japan Meteorological Agency. The threshold of averaged coherence for earthquakes ranging from M2.0 to M4.0 was 0.95 in 1–8 Hz band. For earthquakes larger than M4.0, the frequency band was selected based on the corner frequency of the smaller event (f_0) in the pair. The frequency band extends from ($1/2f_0$) to $2f_0$ and the coherence threshold was 0.8.

The slip for each repeater was estimated based on the following relationship between the seismic moment (M_o; dyne cm) and the fault slip (d; cm) (Nadeau and Johnson, 1998).

$$\log(d) = -2.36 + 0.17\log(M_o) \tag{1}$$

This empirical relationship was obtained from the shallow repeater data for California (Nadeau and Johnson, 1998). Igarashi et al. (2003) have proposed that this relationship is consistent with the slip estimated from the long-term relative plate motion for the repeaters close to the coast of northeastern Japan. The scaling relationships proposed by Nadeau and Johnson (1998) have shown reasonable applicability to several areas (Chen et al., 2007), although regional variations are likely to exist. The seismic moment was estimated from the following relationship between the seismic moment and the magnitude (M).

$$\log(M_o) = 1.5M + 16.1 \tag{2}$$

The magnitude utilized in this study was determined by the Japan Meteorological Agency.

The cumulative slip for each repeating sequence was then calculated by adding the slip amount for each earthquake estimated from equations (1) and (2) (Figs. 3a and b). Subsequently, the average cumulative slip of repeaters was estimated based on sequences within each study area (assuming similar underlying slow-slips) (dashed rectangle in Fig. 3a and timeseries in Fig. 3c). The cumulative slip was detrended (by removing the linear component) for the study period to elucidate temporal fluctuations in the slow-slip (Fig. 3d).

2.2. Long-term SSEs

In the present study, the long-term SSEs catalogue generated by Takagi et al. (2019) was employed. Daily coordinates (F3 solution) were obtained from 330 GEONET stations operated by the Geospatial Information Authority of Japan. Five stations in the Chugoku region were selected as reference stations. Moreover, coseismic offsets of large earthquakes and postseismic deformation due to the 2011 Tohoku-Oki and 2016 Kumamoto earthquakes were removed.

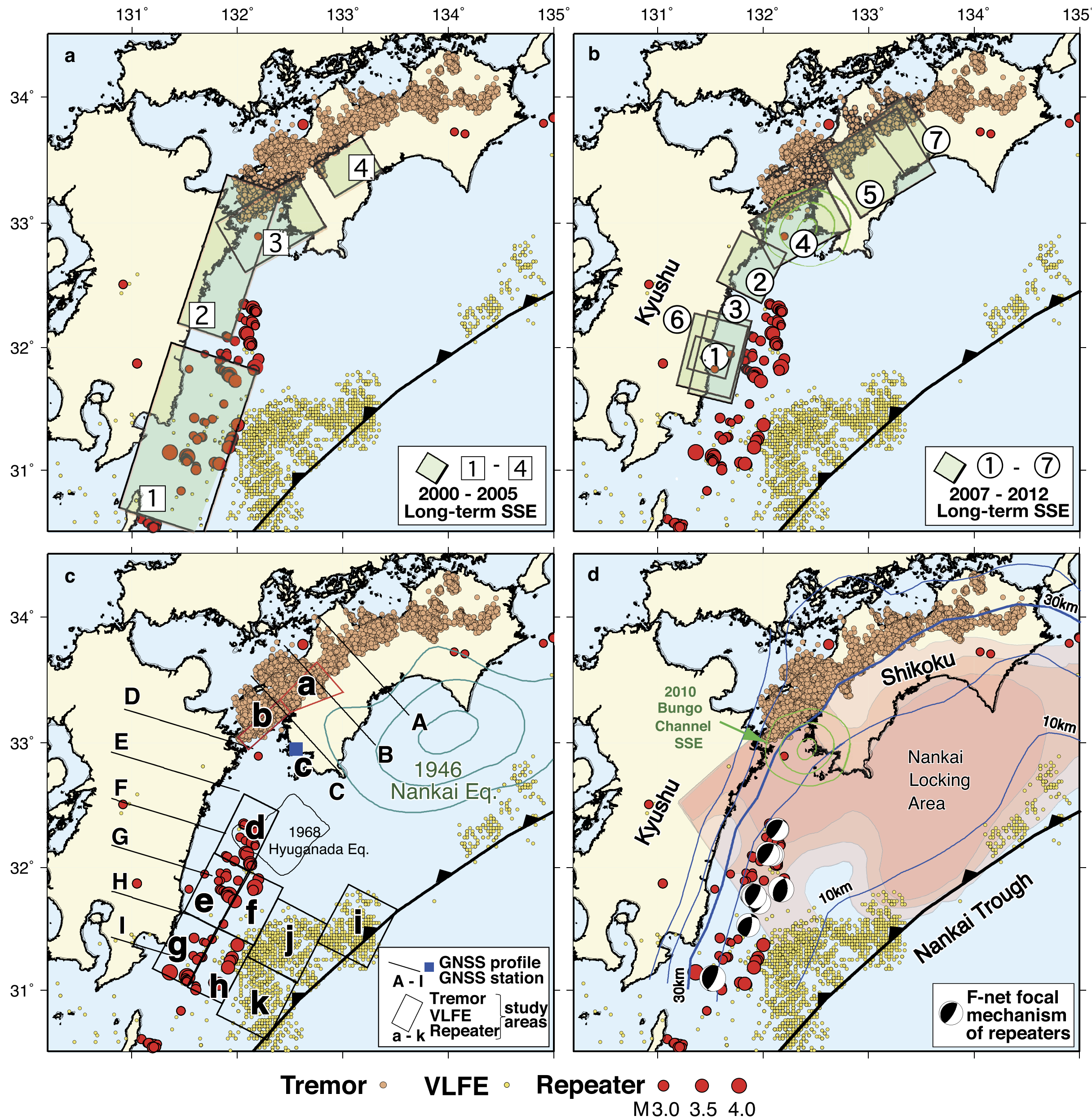

Fig. 2. Distribution of non-volcanic tremors (orange circles), very low frequency earthquakes (yellow circles), and repeating earthquakes (red circles) associated with (a) source areas of long-term SSEs (Takagi et al., 2019) from 2000 to 2005, (b) and from 2007 to 2012; (c) GNSS stacking profiles (from A to I), a GNSS station for the comparison with slow earthquakes (square c) and the study areas for tremor (regions a and b), VLFE (regions i to k), repeaters (regions d to h), and (d) F-net focal mechanisms of repeating earthquakes. In (c), the coseismic slip areas for the 1946 Mw 8.3 Nankai earthquake (Sagiya and Thatcher, 1999) (green contours, denoting 2, 5 and 10 m slips), and for the 1968 M7.5 Hyuga-nada earthquake (Yagi et al., 1998) (black contour) are also shown. In (d), pink shaded colors, green contour lines, and blue contour lines show the slip deficit rate of 3, 4, and 5 cm/year (Yokota et al., 2016), the slip distributions of the 2010 Bungo channel long-term SSE with 10 cm intervals (Geospatial Information Authority of Japan, 2014), and the geometry of the plate interface at 10 km intervals (Baba et al., 2002; Hirose et al., 2008).

The detection algorithm termed as grid-based determination of slow slip events (GriD-SSE) was used for the study. GriD-SSE represents an SSE as a uniform slip on a single rectangular fault and evaluates fitting between observed and modeled displacement time series. The modeled time series are based on the static displacement Green's function and a simple ramp function. The model parameters of the single rectangular faults have been optimized by a nonlinear inversion method. The source locations and onset times were grid searched and a single rectangular fault was estimated by fitting the time series of GNSS displacement. A ramp function was utilized for expressing the temporal evolution of the fault slip. A grid point which maximized variance reduction (VR) in every 0.3° × 0.3° and 100 days and satisfied conditions for detection stability was selected as a candidate for SSE.

2.3. Deep tremors

The occurrence of non-volcanic tremors is usually associated with short-term SSEs and deep VLFEs. This coupling phenomenon is called episodic tremor and slip (ETS) (Rogers and Dragert, 2003; Ito et al., 2007). Because of the sensitivity and detectability, the tremors are considered representative of deep interplate slip. In this study, the tremor catalogue by National Research Institute for Earth Science and Disaster Resilience (2019a) was used for the period from 2003 to 2016, which is an extended catalogue of

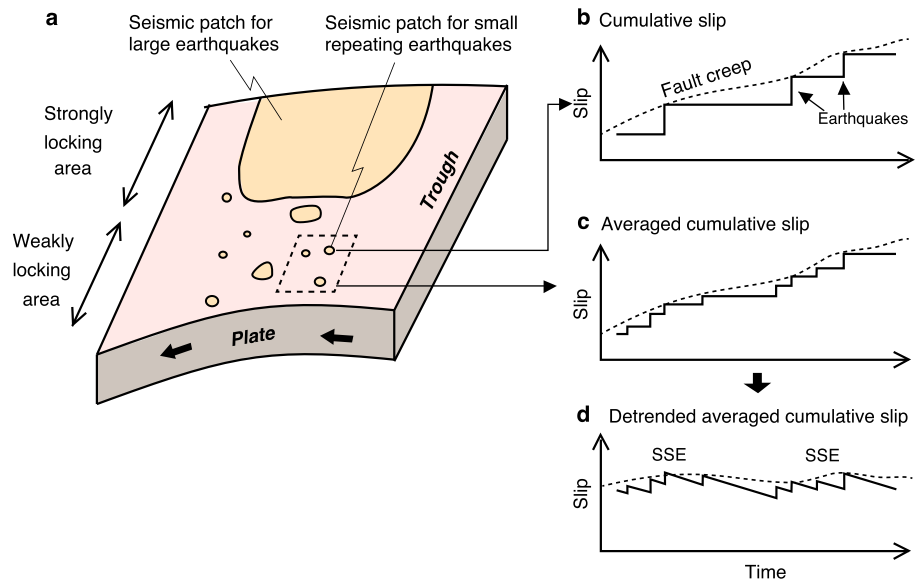

Fig. 3. Schematic representation of repeaters and the procedure for obtaining the detrended average cumulative slip. Repeaters occur where the interplate locking is relatively weak and the fault creep is dominant. Repeaters are considered to occur to catch up with the creep (dashed line) in the surrounding area (a, b). The cumulative slip from multiple repeater sequences was averaged (c) and detrended to identify the SSEs (d).

the one used by Obara et al. (2010). Here the continuous waveform data obtained from the Hi-net (National Research Institute for Earth Science and Disaster Resilience, 2019a) were utilized for the analysis. The centroid locations of the tremors were estimated at one-hour intervals by following the tremor location method proposed by Maeda and Obara (2009). This method is based on the spatial decay of the observed energy of the tremor (estimated from the vertical squared record) and the differential travel time (estimated from the envelope correlation method Obara, 2002).

2.4. Shallow VLFEs

The shallow VLFEs for the period from April 2003 to October 2016 were used in this study which is an extended catalogue of the one used by Asano et al. (2015). Shallow VLFEs and tremors (Yamashita et al., 2015) occur simultaneously probably due to SSEs. Because of the sensitivity and detectability, the VLFEs were considered to be representative of shallow interplate slip. The VLFEs were detected by performing a template search on the stations of Full Range Seismograph Network of Japan (F-net) (National Research Institute for Earth Science and Disaster Resilience, 2019b) as follows. A time series of the cross-correlation (CC) function was calculated for each station from continuous seismograms of four 180 s template VLFEs (after Asano et al., 2015). Assuming a surface wave propagation with a velocity of 3.8 km/s, CCs were back-propagated from the templates to possible origin times and horizontal locations. The time and space domains with grid separations of 1 s and 0.025°, respectively, were utilized to maximize the average CCs across all stations. Grids with averaged CCs greater than 0.5 were selected as possible coherent events. Additionally, only one event was selected as the VLFE candidate when several such events were detected within the 180 s period. If grid points were detected in the same time window from different template events, then the VLFE candidate with the largest average CC (among grid points located within 100 km of the template event) was selected. Regular earthquakes listed in the Japan Meteorological Agency catalogue were removed to construct the final shallow VLFE catalogue.

3. Results

3.1. Spatial distributions of repeaters, long-term SSEs, tremors, VLFEs, and locked areas

Based on the selection of the repeating earthquakes selection, 525 repeaters belonging to 207 sequences (Figs. 2 and 4, Table S1) were identified. The relatively large repeaters displayed interplate type focal mechanism suggesting that they are interplate events (Fig. 2d). The cross-section of the repeater distribution also suggests their location near the plate boundary at the depths ranging 15–30 km (Fig. 4). The discrepancy between the plate model (black line) and the repeater locations could be attributed to systematic location error which occurred due to offshore location of earthquakes (thick black lines) and the depth constraints was not well constrained from land stations. The repeaters were abundant in the southern area (offshore Kyushu) corresponding to the southwest of the source area of the 1946 Nankai earthquake and outside the strongly locked area (Figs. 2c and d), consistent with the mechanism of repeaters that indicate regional fault creep. The long-term SSEs (Figs. 2a and b, rectangles) in Shikoku and the Bungo channel were located at depths of 20–35 km which corresponded to the downdip of the Nankai locked area (Figs. 2c and d). In Kyushu, the depth range of the interplate long-term SSEs was approximately 20–50 km which is the down-dip area of the repeater activities (Figs. 2a and b). Furthermore, 24,720 tremors were identified during the study period (Figs. 2a and b, orange circles). The tremors were active in Shikoku and located at the deeper extension of the long-term SSEs (Fig. 2). The tremors were also considered as interplate events (e.g., Shelly et al., 2006; Ide et al., 2007) and occurred at depths of 30–40 km as suggested by their horizontal locations. Kyushu region did not show active tremor activity, although minor activity was observed downdip of the long-term SSEs (Yabe and Ide, 2013). The shallow VLFEs (Fig. 2, yellow circles) were located at depths ranging 0–15 km depth (offshore Kyushu) and 0–10 km (offshore Shikoku) (Fig. 1). They were located in the updip part of the Nankai locking area offshore Shikoku. In the area of offshore Kyushu, the VLFEs were located updip of the repeater activities.

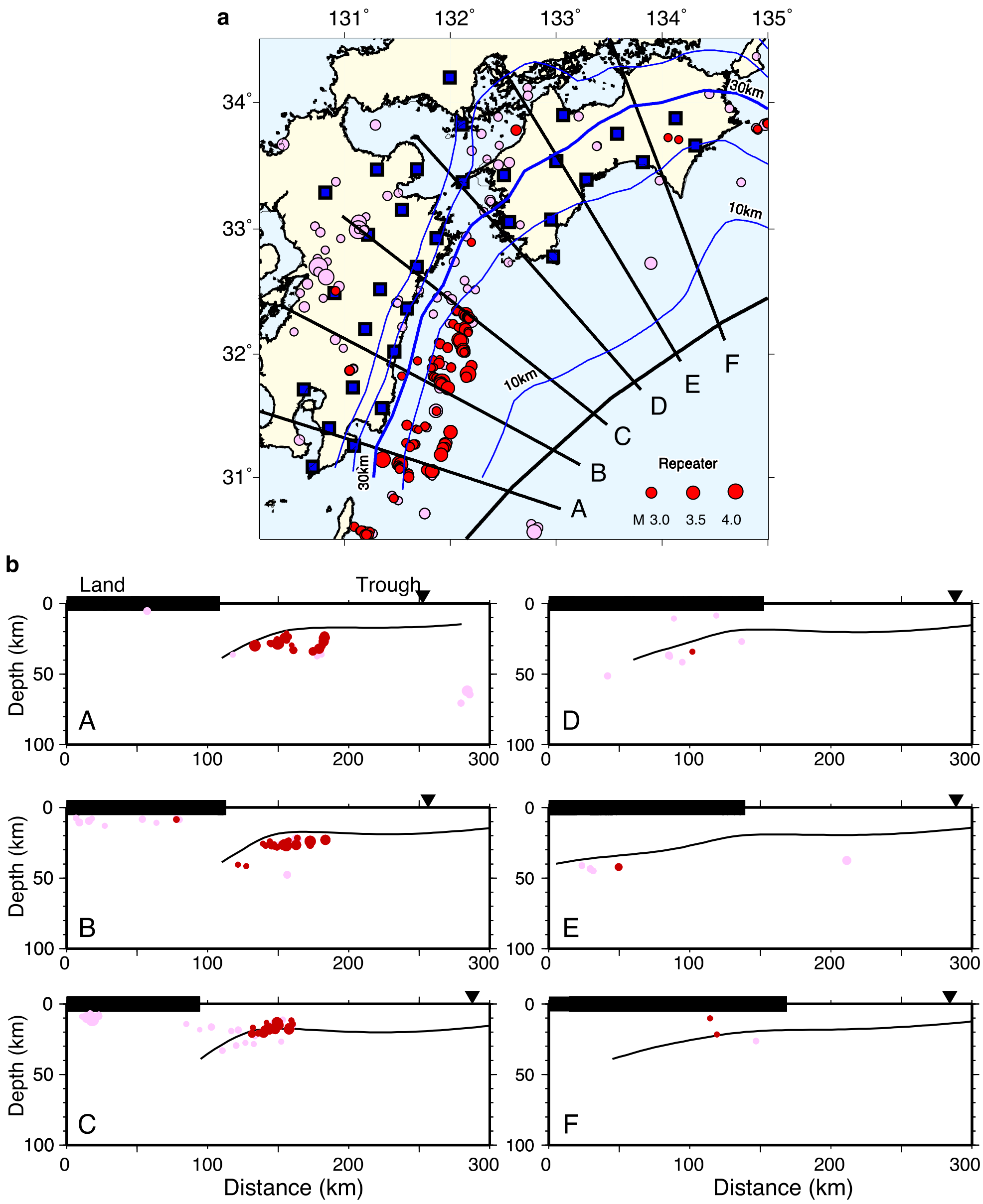

Fig. 4. Spatial distribution of continuous repeaters (red circles) from April 2002 to July 2015. (a) Map view. Epicenters of burst-type sequences (averaged recurrence interval less than 3 years) are indicated by pink circles. Blue squares represent Hi-net stations used to identify the repeaters. (b) Cross-sections along lines A–F presented in panel (a). The lines are taken to the approximate direction of slab dip at depth. The widths of each cross-section is 60 km. Thin lines represent the upper boundary of the Philippine Sea plate (Baba et al., 2002; Hirose et al., 2008). Thick lines and inverted triangles indicate land area and Nankai trough, respectively.

In total, the repeaters, long-term SSEs, deep tremors, shallow VLFEs, and the Nankai locking area were found to be complementarily distributed in space in the southern Nankai subduction zone. These seismic and aseismic events almost covered the entire area in the depth range 0–50 km (offshore Kyushu) and 0–35 km (under Shikoku) along the plate boundary.

3.2. Slow migration of the deep long-term SSEs estimated from repeater, tremor and GNSS data

The previous analysis of GNSS data indicated that the long-term SSEs seem to migrate roughly 50–200 km/year from south to north both before and after the 2003 and 2010 Bungo channel events (Figs. 2a and b) (Takagi et al., 2019). Fig. 5a presents the timing of the SSEs (estimated by Takagi et al., 2019) as inverted triangles in the stacked GNSS displacement time series in the direction parallel to the relative plate motion. The individual timeseries along the observation lines (Fig. S1) also show similar temporal changes for the stations (Fig. S2). Please note that Takagi et al. (2019) used “GriD-SSE” method that utilized spatial pattern of surface displacement to detect long-term SSEs but simple stacking of GNSS time series that we produced for displaying the temporal changes to compare with repeating earthquake and other slow earthquake time series also shows movements probably because all the GNSS stations are located to the west the offshore SSEs. Please see Fig. S3 for the distribution of grid points and Fig. S4 for an example of the detection result by Takagi et al. (2019).

The repeater data shows the occurrence of creep in the repeater distributed area which is located updip of the most GNSS-derived SSE areas (Fig. 2a, b). In this section, we consider repeater sequences only in the offshore Kyushu area where repeaters are occurring along the plate boundary. We set the repeater study areas by dividing the area to shallow and deeper part in dip direc-

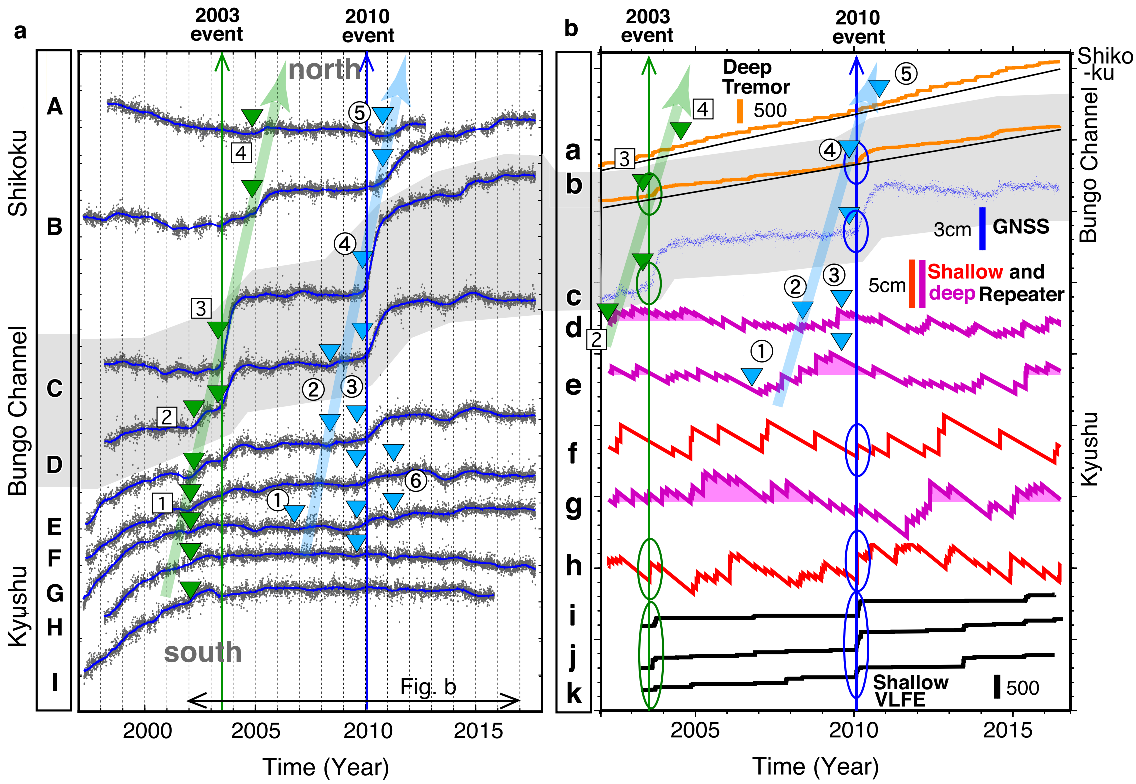

Fig. 5. Temporal changes in seismic and geodetic observations related to the migration of interplate SSEs. (a) Temporal changes in trench-perpendicular surface displacements from GNSS data. The stacked (averaged) GNSS displacements for each profiles A–I (Fig. 2c) are presented. The displacements are parallel component to the profiles and the components of annual variations are removed (Takagi et al., 2019). Blue curves represent moving averages of daily displacements (grey dots). Please refer to Fig. S1 and S2 for the distribution of the GNSS stations and each GNSS time series used for the stacking. (b) Temporal changes in the activities of slow earthquakes and repeater slips. The cumulative number of deep tremors (orange), shallow VLFEs (black) and the detrended cumulative slip of repeaters (red and cyan) for regions a–k (Fig. 2a) are shown. The blue dots are GNSS displacement for station c (Fig. 2c). For both (a) and (b), vertical thin arrows indicate the timings of the long-term SSEs in the Bungo channel. Inverted triangles with squared and circled numbers indicate the starting times of long-term SSEs estimated from the objective search of GNSS data by Takagi et al. (2019) for the period before and after the 2003 event (green) and 2010 event (blue). Numbers correspond to the long-term SSEs presented in Fig. 2. Thick transparent arrows indicate possible slow migrations of long-term SSEs. Green and blue ellipsoids show short-term increases in deep tremor, GNSS displacement, repeater slip and shallow VLFE counts that were likely related to the 2003 (green) and 2010 (blue) Bungo channel events.

tion and three areas in the strike direction of the plate boundary (Fig. 2c). The fluctuations in the detrended cumulative slip show the occurrence of SSEs and provide evidence of SSEs independent from the analysis of GNSS data. The long-term fluctuations in the detrended cumulative slip indicated that the slip amount increase started in 2007 and 2009 in regions e and d, respectively (Fig. 5b). The timings of these increases corresponded to SSE ① and SSE ② detected by Takagi et al. (2019) using GNSS data. It is to be noted that the SSEs timings (reversed triangles in Fig. 5) and locations (rectangles in Fig. 2) are not defined by this study but by Takagi et al. (2019). This enhanced repeater activity in the southern area can also be seen by the snapshot of repeater activities for the period from 2007 to 2009 (Fig. 6f–h). The regions e and d were located in the deeper plate boundary of the repeater-distributed area (Fig. 2c). Additionally, region e distant from the Bungo channel and located to the south) was characterized by early initiation of creep increase (SSE ①). Therefore, the occurrence of the long-term SSEs and their migration to the direction of the 2010 Bungo channel SSE (Hirose et al., 2010) was confirmed by the repeater data. A similar increase in creep was also observed for region d before the occurrence of the 2003 Bungo channel event (SSE $\boxed{2}$) (Hirose et al., 2010) (Fig. 5b, Fig. 6a). However, it is unclear whether the slip rate increase migrated from region e to d due to the limited data period before the 2003 Bungo channel event. For the southern region (region g) and the shallower plate boundary (regions f and h) there was no obvious long-term fluctuation related to the 2003 and 2010 Bungo channel events (Fig. 5b).

Prominent long-term SSEs ($\boxed{3}$ and ④) were observed in the Bungo channel in 2003 and 2010 at the tremor count in region b (Fig. 5b, Fig. 6b and Fig. 6i), GNSS site c (Fig. 5b) and stacked GNSS observations in lines C and D (Fig. 5a). The SSEs migrated further northeast based on the GNSS data (Fig. 5a, Fig. 2, SSEs $\boxed{4}$, ⑤ and ⑦) and tremor count also increased in the same time (Fig. 5b, orange line, Figs. 6b, Figs. 6i–l). Therefore, the results for repeater, deep tremor and GNSS data suggested slow northward migrations of long-term SSEs both before and after the 2003 and 2010 Bungo channel events.

3.3. *Fast migration of the short-term SSEs from VLFE, repeater and tremor data*

Short-term fluctuations around the 2010 Bungo channel event were characterised by slip increases in the repeater time series of regions f and h (Fig. 5b) which were located at the shallow plate boundary of the repeater-distributed area (Fig. 2c). Although the time series for regions f and h indicate several short-term fluctuations, this study focused on the time period before and after the 2010 Bungo channel event. Please note the temporal fluctuations were also observed for the deep and shallow activities of the slow earthquakes occurring in the northern (regions a–c) and southern (regions i–k) areas, respectively (Fig. 5b, blue ellipsoids). Significant short-term changes migrated from the south to the north at a faster speed in contrast to the deep long-term SSE migrations when accounting for the shallow VLFEs

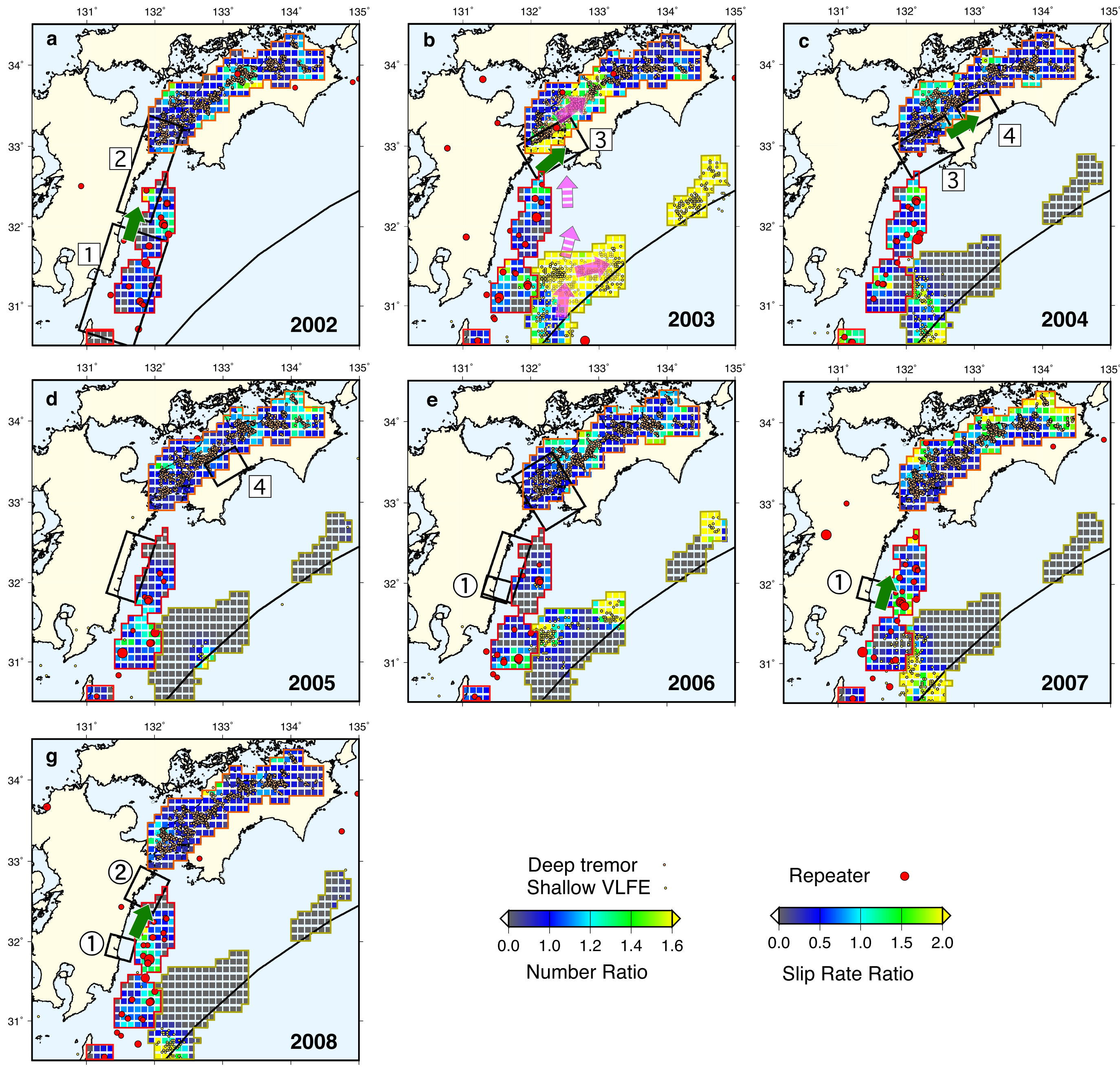

Fig. 6. Spatio-temporal distribution of repeaters (red circles), shallow VLFEs (yellow circles), deep tremors (orange circles), and GNSS-derived long-term SSEs (black rectangles). The event locations are plotted for one-year period shown in the right bottom of each panel. The long-term SSEs were plotted if the SSE duration period overlapped with the year. The colors in the background show averaged number ratios (the number of deep tremors or shallow VLFEs divided by the average number in one year for each phenomenon) and repeater-derived slip rate ratios (the slip rate divided by average slip rate during the entire observation period). The averaging was performed for 0.3° by 0.3° window in latitude and longitude if the number of repeater sequence, VLFEs, and tremors exceeded 4, 20 and 50, respectively. Green and pink arrows indicate slow and fast migration, respectively. The circled and squared numbers show long-term SSEs shown in Figs. 2 a and b that occurred before and after the 2003 and 2010 Bungo channel events, respectively. The SSEs that occurred in 2005 and after 2013 that are not numbered. Areas enclosed by red, yellow and orange lines show the regions where ratios are estimated from repeaters, shallow VLFEs and deep tremors, respectively.

and the deep tremors that activated before and after the repeaters, respectively (Fig. 7b). The snapshot of the activities of repeaters, shallow VLFEs and the deep tremors also show migration of activities although there is relatively large gap of data far offshore Kyushu (dashed arrows, Fig. 8). Since the shallow VLFEs that accompany the tremors are considered to occur due to SSEs (Asano et al., 2015; Yamashita et al., 2015), the short-term changes (including the repeater activity) suggested the occurrence of SSEs. For the 2003 episode the migration of slip increases were not as clear as the 2010 episode but some activities precede the Bungo channel event (Fig. 7a). Please note that the vertical axis of Fig. 7 is not a distance and the migration is not necessarily expressed by a straight line. More evidence is required to test the tendency of northward fast migration. However, the number of steps (short-term changes) during the 15-year analysis period in shallow VLFE, deep tremor, and repeater data are relatively small (Fig. 5b) and the short-term changes occurred within ~1 month which suggest that the coincidence is not likely by chance but there are physical process under the short-term changes.

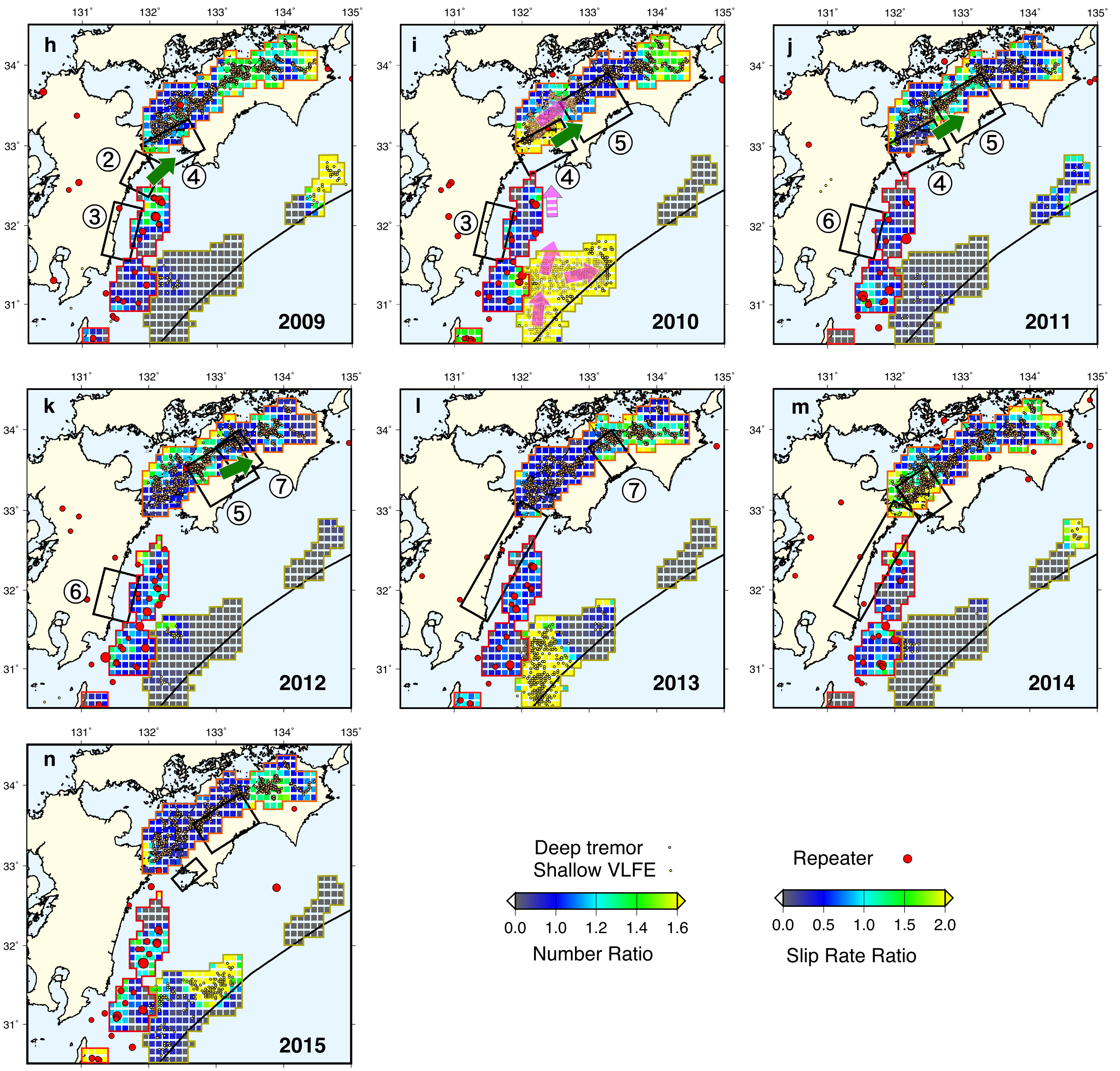

Fig. 6. (*continued*)

4. Discussion

In many subducting plate boundary zones, various migration modes of slow earthquakes have been reported. In the Nankai trough, each kind of slow earthquakes shows its characteristic migration properties. ETS represented by tremor includes three migration modes including along-strike slow-speed migration at velocity of about 10 km/day (Obara, 2002; Dragert et al., 2004), along-strike rapid tremor reversal at velocity of 160–400 km/day (Houston et al., 2011) and along-dip tremor streak at velocity of about 1000 km/day (Shelly et al., 2007; Ghosh et al., 2010). Among these migration modes, the two fastest types of migration modes are observed within each ETS segment. On the other hand, the slow-speed migration of ∼10 km/day propagates to the next segment sometimes (Ito et al., 2007; Obara, 2010). Long-term SSEs beneath Shikoku and Kyushu sometimes propagate to the next segment (Takagi et al., 2016; 2019). The shallow VLFEs and tremors in the southern area offshore Shikoku also show migrations (Asano et al., 2015; Yamashita et al., 2015) (Fig. 1). The results of repeater data and other slow earthquakes suggested that these migrations were connected to each other and indicated widespread migration activity over a wide area (Figs. 5–9). The interactions between different slow earthquakes types probably indicated stress transfer and migration of slow-slips between and within the activity areas. Hirose et al. (2010) suggested the coincidence of the shallow activity of slow earthquakes (VLFEs. Fig. 5, regions i–k), and deep activities of slow earthquakes (Bungo channel long-term SSEs (Fig. 5, region c) and tremors (Fig. 5, regions a, b). However, the closer look of the timing in this study suggest time lag between the shallow and deep phenomena (Fig. 7). The repeaters at the depth in between these shallow VLFEs and deep tremor fill the

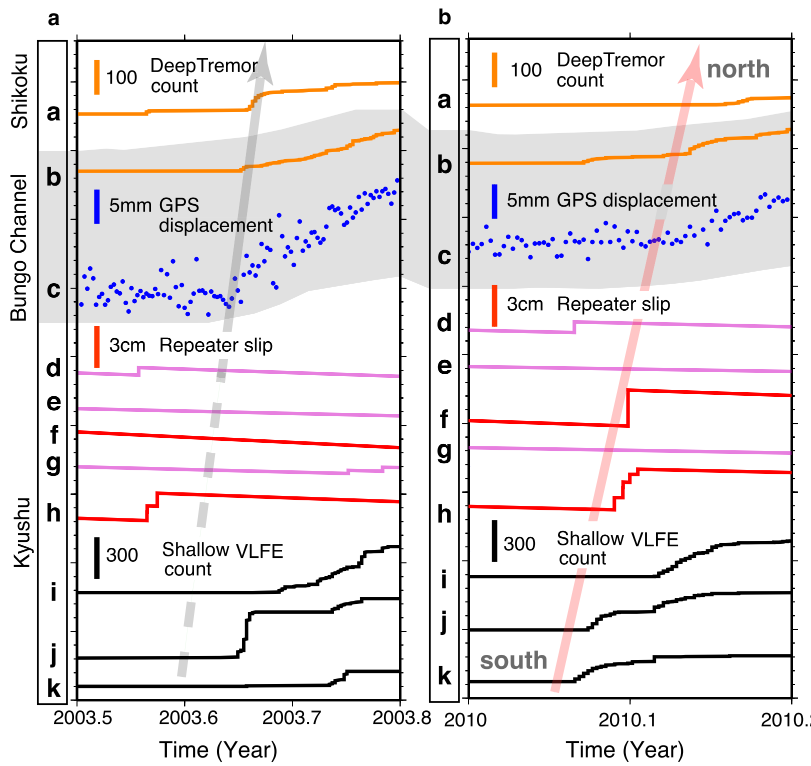

Fig. 7. Temporal changes in the slow earthquake activities, repeater slips, and GNSS displacements for the 2003 and 2010 episodes. This figure is the same as Fig. 5(b) except for the time range. Thick arrows indicate possible fast migrations of the SSEs. Note different time scales in panels (a) and (b).

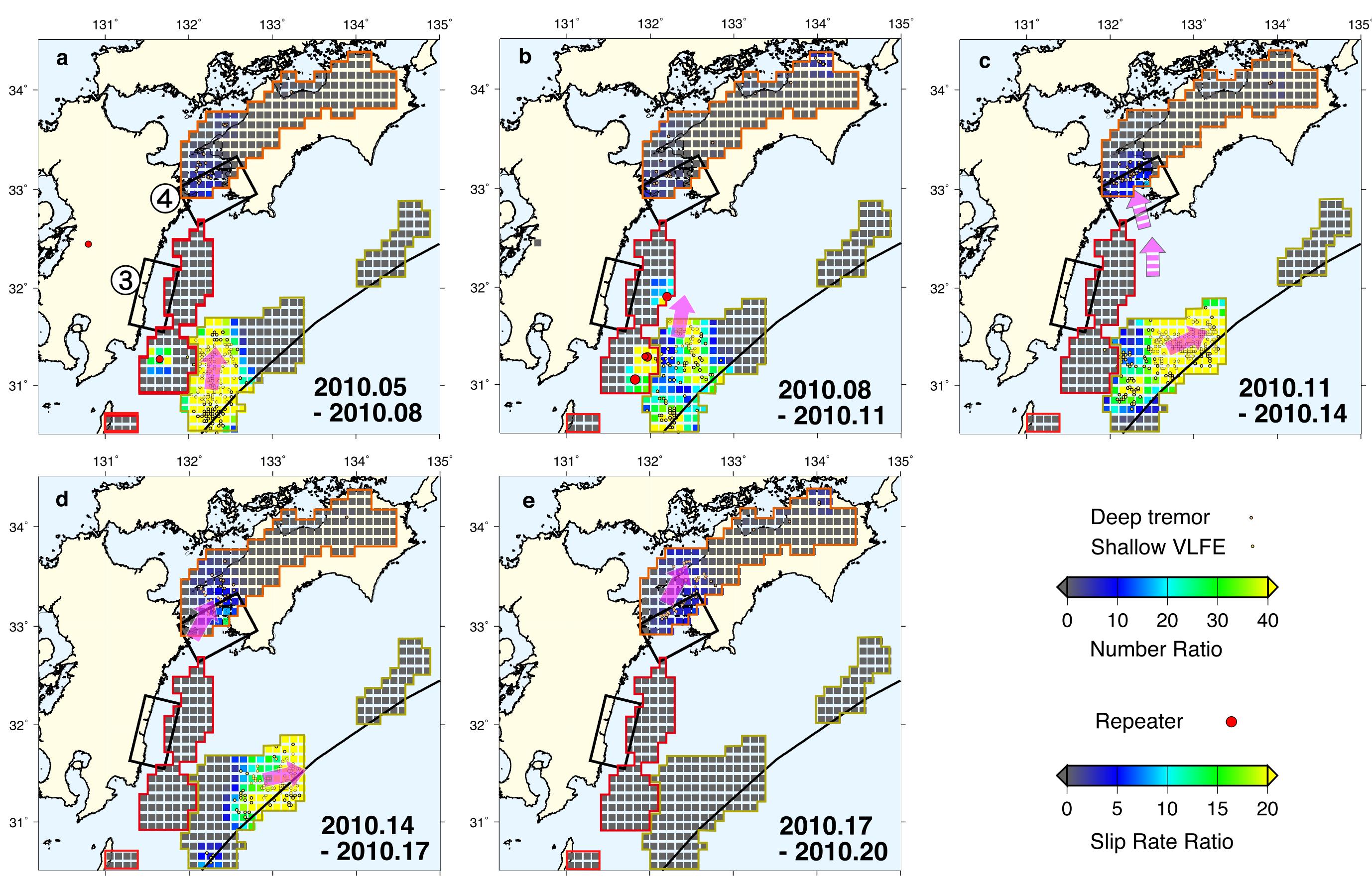

Fig. 8. The same as Fig. 6 but for the period from 2010.05 to 2010.20 in short (0.03 year) intervals. Please note a different color scale from that in Fig. 6. Pink arrows represent fast migration of slow slips.

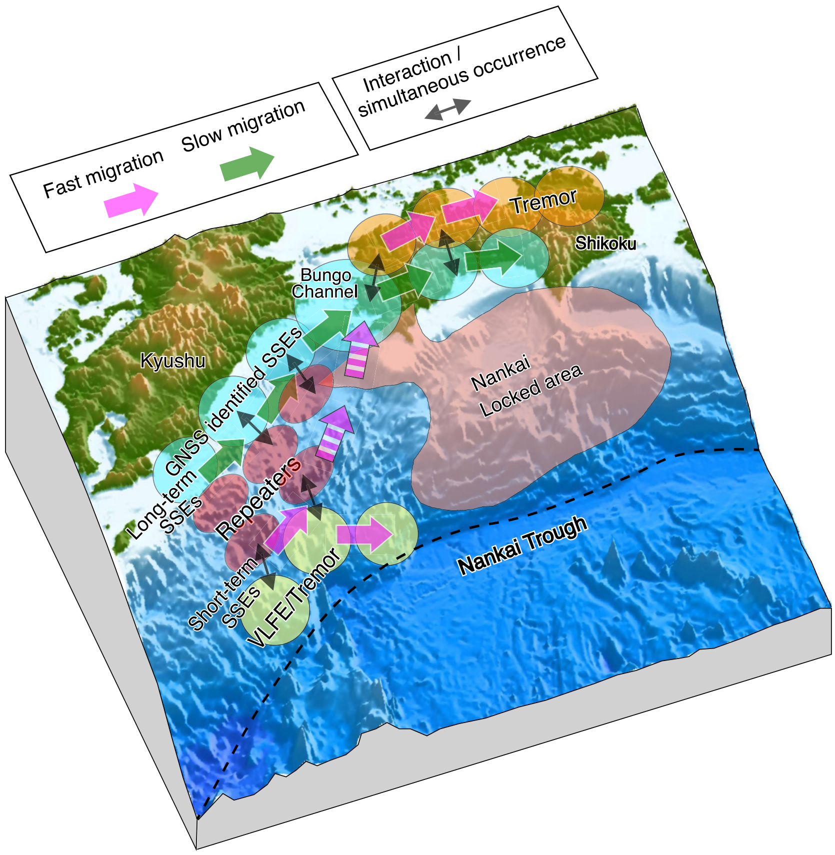

Fig. 9. Schematic showing the locations of the locking area, long-term SSEs, deep tremors, VLFEs, and repeaters together with the migration of the activities. Different types of slow earthquakes and repeaters are complementarily distributed. Black arrows show interactions between activities. Pink and green arrows respectively show fast and slow migrations of the SSEs. Pink arrows with stripe offshore the Bungo channel show a possible migration where no SSE was observed in the present dataset. Dashed black line shows the location of the Nankai trough. The difference from Fig. 1 is the data of repeaters and the interactions (double headed arrows) between different kinds of activities.

gap in time and space (Fig. 7). The repeaters and slow earthquakes suggested fast migrations of SSEs to the north. The short-term SSEs traveled approximately 300 km over a period of 30 days (10 km/day) in 2015 and this speed was similar to the one observed for deep tremors (Obara, 2010) and shallow VLFEs (Sugioka et al., 2012). Clear slip increases were not observed in this study from the repeaters for the 2003 episode (Fig. 5b). This suggests the slip migrated in the shallower plate boundary than the short-term SSE during the 2010 episode that activated deep repeating earthquakes.

The deep slow and shallow fast SSE migrations indicated movement towards the Bungo channel and further north. The "along trough" direction of movements corresponded to the direction from the weakly coupled southern area to strongly locked northern area (Figs. 1 and 9). The SSEs are often observed around the locked area of the plate boundary (Obara and Kato, 2016). Migrations of SSEs to the future hypocenters and/or locked areas have been observed for the 2011 Tohoku-oki (Kato et al., 2012) and the 2014 Iquique earthquakes (Kato and Nakagawa, 2014). Multiple migrations of seismicity toward the center of the locking region have also been reported at the small scale for the Kamaishi repeater, NE Japan (Uchida et al., 2012). Previous earthquake simulations have also suggested the occurrence of SSE migrations, shrinkage of the locked area, and frequent SSEs during the late stage of an earthquake cycle (Ariyoshi et al., 2012; Cattania and Segall, 2019; Jiang and Lapusta, 2017; Ohtani et al., 2014) although these phenomena may depend on the assumed frictional properties. The directivity of the migration may reflect the spatial distribution of the locking and the stressing conditions to the locked area along the Nankai trough. It is difficult to explain the migrations by local processes such as fluid migration given the large spatial scale (∼300 km) even though the migrations within each phenomenon (repeaters, tremors, etc.) can be related to such processes. Conversely, the interaction between the slow earthquakes and the large migration scale suggests that they behave as a single system that may be related to the deformation of the subducting slab. Considering the spatial scale of the locked area of the Nankai earthquake (∼300 km along the trough), it is likely that the migrations were related to the unfastening of the locked area of the Nankai earthquake.

5. Conclusions

In this study, newly identified small repeating earthquakes and existing/updated slow earthquake catalogs along the south Nankai trough have been examined to understand their spatio-temporal relationships. The results indicated that these phenomena were complementarily distributed in space, thus suggesting different frictional properties for the areas producing these activities. The temporal distribution of the slow earthquakes (shallow VLFEs, deep tremors and long-term SSEs) and repeaters revealed interactions between different kind of slow earthquakes. The activities indicated northward migration along the ∼300 km plate boundary before and after the 2003 and 2010 Bungo-channel SSEs. The migrations occurred slowly (over a period of several years) at the deep plate boundary (depth $\geq$ 20 km) and faster (∼1 month) at the shallow to deep (0–50 km) plate boundary. The migrations were widespread over the transitional area between the locked and weakly coupled regions along the plate boundary, thus suggesting that the phenomena were related to the unlocking of the interplate locked area offshore Shikoku. The results also suggested the occurrence of non-steady stressing in the locked area along the plate boundary during the interseismic period.

Declaration of competing interest

The authors declare that they have no known competing financial interests or personal relationships that could have appeared to influence the work reported in this paper.

Acknowledgements

We used the Japan Meteorological Agency (JMA) earthquake and F-net focal mechanism catalogues. The repeating earthquakes were selected based on the seismic waveforms from Hi-net stations operated by the National Research Institute for Earth Science and Disaster Resilience. This research was supported by JSPS KAKENHI Grant Number JP16H06473 and JP16H06474 in Scientific Research on Innovative Areas "Science of Slow Earthquakes". This work was also supported in part by JSPS KAKENHI 15K05260, 17H05309 and ERI JURP 2017-G-05. We thank J. Jara and two anonymous reviewers for helpful comments, H. Tsuruoka and S. Nakagawa for the waveform database and R. Burgmann for discussion.

Appendix A. Supplementary material

Supplementary material related to this article can be found online at https://doi.org/10.1016/j.epsl.2019.115986.

References

Ando, M., 1975. Source mechanisms and tectonic significance of historical earthquakes along the nankai trough, Japan. Tectonophysics 27, 119–140. https://doi.org/10.1016/0040-1951(75)90102-X.

Ariyoshi, K., Matsuzawa, T., Ampuero, J.-P., Nakata, R., Hori, T., Kaneda, Y., Hino, R., Hasegawa, A., 2012. Migration process of very low-frequency events based on a chain-reaction model and its application to the detection of preseismic slip for megathrust earthquakes. Earth Planets Space 64, 693–702. https://doi.org/10.5047/eps.2010.09.003.

Asano, Y., Obara, K., Matsuzawa, T., Hirose, H., Ito, Y., 2015. Possible shallow slow-slip events in Hyuga-nada, Nankai subduction zone, inferred from migration of very low frequency earthquakes. Geophys. Res. Lett. 42, 331–338. https://doi.org/10.1002/2014GL062165.

Baba, T., Tanioka, Y., Cummins, P.R., Uhira, K., 2002. The slip distribution of the 1946 Nankai earthquake estimated from tsunami inversion using a new plate model. Phys. Earth Planet. Inter. 132, 59–73. https://doi.org/10.1016/S0031-9201(02)00044-4.

Beroza, G.C., Ide, S., 2011. Slow earthquakes and nonvolcanic tremor. Annu. Rev. Earth Planet. Sci. 39, 271–296. https://doi.org/10.1146/annurev-earth-040809-152531.

Bürgmann, R., 2018. The geophysics, geology and mechanics of slow fault slip. Earth Planet. Sci. Lett. 495, 112–134. https://doi.org/10.1016/j.epsl.2018.04.062.

Cattania, C., Segall, P., 2019. Crack models of repeating earthquakes predict observed moment-recurrence scaling. J. Geophys. Res., Solid Earth 124, 476–503. https://doi.org/10.1029/2018JB016056.

Chen, K.H., Nadeau, R.M., Rau, R.J., 2007. Towards a universal rule on the recurrence interval scaling of repeating earthquakes? Geophys. Res. Lett. 34. https://doi.org/10.1029/2007GL030554.

Dragert, H., Wang, K., Rogers, G., 2004. Geodetic and seismic signatures of episodic tremor and slip in the northern Cascadia subduction zone. Earth Planets Space 56, 1143–1150.

Geospatial Information Authority of Japan, 2014. Crustal deformation in October 2014. http://www.gsi.go.jp/common/000097569.pdf.

Ghosh, A., Vidale, J.E., Sweet, J.R., Creager, K.C., Wech, A.G., Houston, H., Brodsky, E.E., 2010. Rapid, continuous streaking of tremor in Cascadia. Geochem. Geophys. Geosyst. 11, Q12010.

Graham, S.E., DeMets, C., Cabral-Cano, E., Kostoglodov, V., Walpersdorf, A., Cotte, N., Brudzinski, M., McCaffrey, R., Salazar-Tlaczani, L., 2014. GPS constraints on the 2011–2012 Oaxaca slow slip event that preceded the 2012 March 20 Ometepec earthquake, southern Mexico. Geophys. J. Int. 197, 1593–1607. https://doi.org/10.1093/gji/ggu019.

Hirose, F., Nakajima, J., Hasegawa, A., 2008. Three-dimensional seismic velocity structure and configuration of the Philippine Sea slab in southwestern Japan estimated by double-difference tomography. J. Geophys. Res., Solid Earth 113, B09315. https://doi.org/10.1029/2007JB005274.

Hirose, H., Asano, Y., Obara, K., Kimura, T., Matsuzawa, T., Tanaka, S., Maeda, T., 2010. Slow earthquakes linked along dip in the nankai subduction zone. Science 330, 1502. https://doi.org/10.1126/science.1197102.

Hirose, H., Obara, K., 2005. Repeating short- and long-term slow-slip events with deep tremor activity around the Bungo channel region, southwest Japan. Earth Planets Space 57, 961–972. https://doi.org/10.1186/BF03351875.

Ide, S., Shelly, D.R., Beroza, G.C., 2007. Mechanism of deep low frequency earthquakes: further evidence that deep non-volcanic tremor is generated by shear slip on the plate interface. 34, L03308. https://doi.org/10.1029/2006GL028890.

Igarashi, T., Matsuzawa, T., Hasegawa, A., 2003. Repeating earthquakes and interplate aseismic slip in the northeastern Japan subduction zone. J. Geophys. Res., Solid Earth 108. https://doi.org/10.1029/2002JB001920.

Ito, Y., Obara, K., Shiomi, K., Sekine, S., Hirose, H., 2007. Slow earthquakes coincident with episodic tremors and slow slip events. Science 315, 503–506.

Houston, H., Delbridge, B.G., Wech, A.G., Creager, K.C., 2011. Rapid tremor reversals in Cascadia generated by a weakened plate interface. Nat. Geosci. 4, 404.

Jiang, J., Lapusta, N., 2017. Connecting depth limits of interseismic locking, microseismicity, and large earthquakes in models of long-term fault slip. J. Geophys. Res., Solid Earth 122, 6491–6523. https://doi.org/10.1002/2017JB014030.

Kato, A., Nakagawa, S., 2014. Multiple slow-slip events during a foreshock sequence of the 2014 Iquique, Chile Mw 8.1 earthquake. Geophys. Res. Lett. 41, 5420–5427. https://doi.org/10.1002/2014GL061138.

Kato, A., Obara, K., Igarashi, T., Tsuruoka, H., Nakagawa, S., Hirata, N., 2012. Propagation of slow slip leading up to the 2011 Mw 9.0 Tohoku-Oki earthquake. Science 335, 705–708. https://doi.org/10.1126/science.1215141.

Maeda, T., Obara, K., 2009. Spatiotemporal distribution of seismic energy radiation from low-frequency tremor in western Shikoku, Japan. J. Geophys. Res., Solid Earth 114, B00A09. https://doi.org/10.1029/2008JB006043.

Matsuzawa, T., Hirose, H., Shibazaki, B., Obara, K., 2010. Modeling short- and long-term slow slip events in the seismic cycles of large subduction earthquakes. 115. https://doi.org/10.1029/2010JB007566.

Mavrommatis, A.P., Segall, P., Uchida, N., Johnson, K.M., 2015. Long-term acceleration of aseismic slip preceding the Mw 9 Tohoku-oki earthquake: constraints from repeating earthquakes. Geophys. Res. Lett. 42, 9717–9725. https://doi.org/10.1002/2015GL066069.

Mazzotti, S., Adams, J., 2004. Variability of near-term probability for the next great earthquake on the Cascadia subduction zone. Bull. Seismol. Soc. Am. 94, 1954–1959. https://doi.org/10.1785/012004032.

Meng, L., Huang, H., Bürgmann, R., Ampuero, J.P., Strader, A., 2015. Dual megathrust slip behaviors of the 2014 Iquique earthquake sequence. Earth Planet. Sci. Lett. 411, 177–187. https://doi.org/10.1016/j.epsl.2014.11.041.

Nadeau, R.M., Johnson, L.R., 1998. Seismological studies at Parkfield VI: moment release rates and estimates of source parameters for small repeating earthquakes. Bull. Seismol. Soc. Am. 88, 790–814.

National Research Institute for Earth Science and Disaster Resilience, 2019a. NIED Hi-net. National Research Institute for Earth Science and Disaster Resilience.

National Research Institute for Earth Science and Disaster Resilience, 2019b. NIED F-net. National Research Institute for Earth Science and Disaster Resilience.

Nishimura, T., Yokota, Y., Tadokoro, K., Ochi, T., 2018. Strain partitioning and interplate coupling along the northern margin of the Philippine Sea plate, estimated from Global Navigation Satellite System and Global Positioning System-Acoustic data. Geosphere 14, 535–551. https://doi.org/10.1130/GES01529.1.

Obara, K., 2002. Nonvolcanic deep tremor associated with subduction in southwest Japan. Science 296, 1679–1681.

Obara, K., 2010. Phenomenology of deep slow earthquake family in southwest Japan: spatiotemporal characteristics and segmentation. J. Geophys. Res., Solid Earth 115, B00A25. https://doi.org/10.1029/2008JB006048.

Obara, K., Kato, A., 2016. Connecting slow earthquakes to huge earthquakes. Science 353, 253–257. https://doi.org/10.1126/science.aaf1512.

Obara, K., Tanaka, S., Maeda, T., Matsuzawa, T., 2010. Depth-dependent activity of non-volcanic tremor in southwest Japan. Geophys. Res. Lett. 37, L13306. https://doi.org/10.1029/2010GL043679.

Ohtani, M., Hirahara, K., Hori, T., Hyodo, M., 2014. Observed change in plate coupling close to the rupture initiation area before the occurrence of the 2011 Tohoku earthquake: implications from an earthquake cycle model. Geophys. Res. Lett. 41, 1899–1906. https://doi.org/10.1002/2013GL058751.

Radiguet, M., Perfettini, H., Cotte, N., Gualandi, A., Valette, B., Kostoglodov, V., Lhomme, T., Walpersdorf, A., Cabral Cano, E., Campillo, M., 2016. Triggering of the 2014 Mw7.3 Papanoa earthquake by a slow slip event in Guerrero, Mexico. Nat. Geosci. 9, 829.

Roeloffs, E.A., 2006. Evidence for aseismic deformation rate changes prior to earthquakes. Annu. Rev. Earth Planet. Sci. 34, 591–627. https://doi.org/10.1146/annurev.earth.34.031405.124947.

Rogers, G., Dragert, H., 2003. Episodic tremor and slip on the Cascadia subduction zone: the chatter of silent slip. Science 300, 1942–1943.

Sagiya, T., Thatcher, W., 1999. Coseismic slip resolution along a plate boundary megathrust: the Nankai Trough, southwest Japan. J. Geophys. Res., Solid Earth 104, 1111–1129. https://doi.org/10.1029/98jb02644.

Segall, P., Bradley, A.M., 2012. Slow-slip evolves into megathrust earthquakes in 2D numerical simulations. Geophys. Res. Lett. 39, L18308. https://doi.org/10.1029/2012GL052811.

Shelly, D.R., Beroza, G.C., Ide, S., 2007. Non-volcanic tremor and low-frequency earthquake swarms. Nature 446, 305. https://doi.org/10.1038/nature05666.

Shelly, D.R., Beroza, G.C., Ide, S., Nakamula, S., 2006. Low-frequency earthquakes in Shikoku, Japan, and their relationship to episodic tremor and slip. Nature 442, 188–191. https://doi.org/10.1038/nature04931.

Sugioka, H., Okamoto, T., Nakamura, T., Ishihara, Y., Ito, A., Obana, K., Kinoshita, M., Nakahigashi, K., Shinohara, M., Fukao, Y., 2012. Tsunamigenic potential of the shallow subduction plate boundary inferred from slow seismic slip. Nat. Geosci. 5, 414–418. https://doi.org/10.1038/ngeo1466.

Takagi, R., Obara, K., Maeda, T., 2016. Slow-slip event within a gap between tremor and locked zones in the Nankai subduction zone. Geophys. Res. Lett. 43, 1066–1074. https://doi.org/10.1002/2015GL066987.

Takagi, R., Uchida, N., Obara, K., 2019. Along-strike variation and migration of long-term slow-slip events in the western Nankai subduction zone, Japan. J. Geophys. Res., Solid Earth 124. https://doi.org/10.1029/2018JB016738.

Uchida, N., Bürgmann, R., 2019. Repeating earthquakes. Annu. Rev. Earth Planet. Sci. 47, 305–332. https://doi.org/10.1146/annurev-earth-053018-060119.

Uchida, N., Iinuma, T., Nadeau, R.M., Bürgmann, R., Hino, R., 2016. Periodic slow-slip triggers megathrust zone earthquakes in northeastern Japan. Science 351, 488–492. https://doi.org/10.1126/science.aad3108.

Uchida, N., Matsuzawa, T., 2013. Pre- and postseismic slow-slip surrounding the 2011 Tohoku-oki earthquake rupture. Earth Planet. Sci. Lett. 374, 81–91. https://doi.org/10.1016/j.epsl.2013.05.021.

Uchida, N., Matsuzawa, T., Ellsworth, W.L., Imanishi, K., Shimamura, K., Hasegawa, A., 2012. Source parameters of microearthquakes on an interplate asperity off Kamaishi, NE Japan over two earthquake cycles. Geophys. J. Int. 189, 999–1014. https://doi.org/10.1111/j.1365-246X.2012.05377.x.

Voss, N., Dixon, T.H., Liu, Z., Malservisi, R., Protti, M., Schwartz, S., 2018. Do slow slip events trigger large and great megathrust earthquakes? 4, eaat8472. https://doi.org/10.1126/sciadv.aat8472.

Yabe, S., Ide, S., 2013. Repeating deep tremors on the plate interface beneath Kyushu, southwest Japan. Earth Planets Space 65, 17–23. https://doi.org/10.5047/eps.2012.06.001.

Yagi, Y., Kikuchi, M., Yoshida, S., Yamanaka, Y., 1998. Source process of the Hyuuga-nada earthquake of April 1, 1968 (M_{JMA} 7.5), and its relationship to the subsequent seismicity. J. Seismol. Soc. Jpn. 51, 139–148. https://doi.org/10.4294/zisin1948.51.1_139.

Yamashita, Y., Shimizu, H., Goto, K., 2012. Small repeating earthquake activity, interplate quasi-static slip, and interplate coupling in the Hyuga-nada, southwestern Japan subduction zone. Geophys. Res. Lett. 39, L08304. https://doi.org/10.1029/2012GL051476.

Yamashita, Y., Yakiwara, H., Asano, Y., Shimizu, H., Uchida, K., Hirano, S., Umakoshi, K., Miyamachi, H., Nakamoto, M., Fukui, M., Kamizono, M., Kanehara, H., Yamada, T., Shinohara, M., Obara, K., 2015. Migrating tremor off southern Kyushu as evidence for slow-slip of a shallow subduction interface. Science 348, 676–679. https://doi.org/10.1126/science.aaa4242.

Yokota, Y., Ishikawa, T., Watanabe, S.I., Tashiro, T., Asada, A., 2016. Seafloor geodetic constraints on interplate coupling of the Nankai Trough megathrust zone. Nature 534, 374–377. https://doi.org/10.1038/nature17632.